OPTOELECTRONICS AND ADVANCED MATERIALS – RAPID COMMUNICATIONS Vol. 2, No. 10, October 2008, p. 635 - 639

# Effect of composition on optical constants of Pb: GeSbTe chalcogenide thin films

J. KUMAR, P. KUMAR, N. SURI, M. AHMAD, R. THANGARAJ*, T. STEPHEN SATHIARAJ[a]
*Semiconductors Laboratory, Department of Applied Physics, Guru Nanak Dev Univeristy, Amritsar-143005, India*
*[a]Department of Physics, University of Botswana, Botswana*

Optical properties of Pb doped ternary Ge-Sb-Te chalcognide films prepared by thermal evaporation have been studied in the visible and near-infrared spectral regions. The straightforward analysis proposed by Swanepoel has been successfully employed and it has allowed us to accurately determine the refractive index and extinction coefficient of the films. The refractive index has been determined from the upper and lower envelopes of the transmission spectra. The absorption coefficient and extinction coefficient have been determined from the transmission spectra in the strong-absorption region. The dispersion of the refractive index is discussed in terms of the Wemple–DiDomenico single oscillator model.

(Received August 1, 2008; accepted August 14, 2008)

*Keywords*: Chalcogenide; Thin films; Optical properties; $Ge_2Sb_2Te_5$ (GST)

## 1. Introduction

Amorphous chalcogenide glasses form an interesting class of non-crystalline materials owing to their excellent transmittance in infrared region, continuous shift of optical-absorption edge, large reflectivity difference between amorphous and crystalline states and high refractive index. The correlation between the above properties with chemical composition enable us to tailor these materials for use in optical fibers, filters, anti-reflection coatings, data storage devices and a wide variety of optical devices [1-4]. The range of photo-induced changes that chalcogenide glasses exhibit such as photodecomposition, photocrystallisation, photoinduced morphological changes, photovaporisation, photopolymerisation, photodissolution of certain metals and photovitrification, light-induced changes in local atomic configuration and absorption-edge shifts, offers possibility of using these materials in the fabrication of various optical devices [5]. In general, these phenomena are associated with significant changes in the optical constants. Therefore, the accurate determination of the optical constants of these materials with a simple technique is important, not only in order to know the basic mechanisms underlying these phenomena, but also to exploit and develop them for interesting technological applications.

Recently, stoichiometric ternary chalcogenide alloys based on Ge-Sb-Te have been successfully applied in commercial optical disk for data storage [6]. $Ge_2Sb_2Te_5$ (GST) is of great interest because of its extensive use in phase change memories [6, 7]. Due to its (i) faster crystallization, (ii) reflectivity and large resistivity difference between amorphous and crystalline states, GST finds application in DVD-RAM and PCRAM [3, 4, 8]. Amorphous-crystalline transformation in GST is fast and stable due to the absence of the rupture of strong covalent bonds during the above process. The Te sub lattice as well as the structure around Sb atoms is partially preserved in the amorphous state [9]. Several workers have reported the impurity effects on $Ge_2Sb_2Te_5$ alloy [8, 10-13]. Impurity addition in $Ge_2Sb_2Te_5$ alloy has importance in fabrication of materials with desirable phase change properties.

Swanepoel's method for determining the optical constants, using only the transmission spectra, is particularly useful because it accounts for a possible lack of film-thickness uniformity [14]. This method is based on the upper and lower envelopes of normal-incidence optical transmission spectra and takes into account the spectrum compression, i.e., increase of minima and decrease of maxima of interference caused by film-thickness variations across the light spot defined by the spectrophotometer beam. In the present work, a systematic study on the effect of composition in Pb doped $Ge_2Sb_2Te_5$ system on the optical constants calculated using Swanepoel method has been carried out.

## 2. Experimental

Bulk $Pb_xGe_{22-x}Sb_{22}Te_{55}$ (x = 0, 1, 3) alloys were prepared by melt quenching technique. The constituent elements (99.999% purity) were weighed according to their atomic percentage and were sealed in a quartz ampoule (length ~10 cm, internal diameter ~6 mm), in a vacuum of $\sim 10^{-5}$ mbar. The sealed ampoule was kept in a vertical furnace for 48 h and the temperature was raised to 1000 °C, at a rate of 4-5°C/min. The ampoule was rocked constantly to ensure homogeneous mixing of the melt. Finally, the ampoule containing molten alloy was quenched in ice-cold water. The bulk material was extracted from quartz ampoule by dissolving the ampoule in $HF+H_2O_2$ solution for about 48 h. Ingot so obtained was crushed into fine powder.

Thin films of the above-mentioned Pb:GeSbTe alloys were prepared by thermal evaporation method using Hind High Vacuum Coating Unit (Model No. 12A4D). Well-cleaned glass slides were used as substrates. The substrates were maintained at room temperature during deposition and the pressure in the chamber during the deposition was below $10^{-5}$ mbar. The films were left inside the vacuum chamber after deposition for ~24 h to attain metastable equilibrium as suggested by Abkowitz [15]. The chemical compositions were determined using EDAX attached with Scanning Electron Microscope (Philips XL 30 ESEM system). The average composition of each thin film was obtained by measuring three regions of the thin film. The transmittance ($T$) w.r.t. air and specular reflectance ($R$) of thin films were measured at room temperature using UV-VIS-NIR spectrophotometer (VARIAN Cary 500) in the wavelength range 200-3000nm.

## 3. Results

*Refractive index and extinction coefficient*

Fig. 1 shows the variation of optical transmission ($T$) with wavelength ($\lambda$) in $Pb_0Ge_{20}Sb_{24}Te_{56}$, $Pb_{1.6}Ge_{19}Sb_{26}Te_{54}$ and $Pb_5Ge_{12}Sb_{28}Te_{55}$ thin films. The fringes shown in the plot are formed due to constructive and destructive interference of light reflected from the surface and film-substrate interface. In the region of fringes the film behaves as partial transparent film. The small fringe amplitude represents the strong absorption, amplitude close to maxima represents medium absorption and the parallel set of maxima and minima represent completely a transparent wavelength region. The parabolic interpolation of neighboring extremes has been carried out to determine the maximum and minimum envelopes $T_M$ ($\lambda$) and $T_m$ ($\lambda$) respectively in the transparent region. The set of maxima and minima so obtained were used to calculate refractive index $n_1$ and variation in thickness $\int d$, in transparent region using transcendental equations given by Swanepoel [14] with the help of Newton-Raphson iterative method.

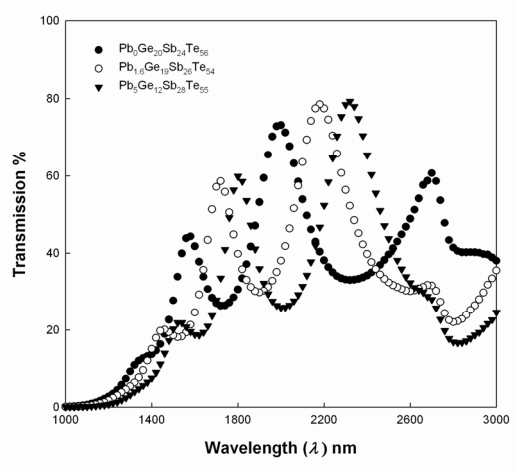


*Fig. 1. Transmission spectra for Pb:GeSbTe chalcogenide thin films.*

The thin film thickness $d$ measured using surface profiler (Table 1) were used to calculate the 'order of interference' $m_0$, using relation $2nd = m\lambda$. The accuracy of the film thickness and hence the accuracy of the refractive index is significantly increased by taking the corresponding exact integer or half integer value of m. Then $d_1$ and m were then used to calculate the final refractive index value n. The values of $m_0$, m and $d_1$ are also listed in Table 1.

*Table 1. Values of $\lambda$, $T_M$, $T_m$, d and n for the three different composition of Pb:GeSbTe thin films.*

| $\lambda$ [nm] | $T_M$ | $T_m$ | $\int_d$ [nm] | $n_1$ | $m_0$ | $m$ | $n$ |
|---|---|---|---|---|---|---|---|
| $Pb_0Ge_{20}Sb_{24}Te_{56}$ | | | | | | | |
| 2321 | 0.734 | 0.330 | 61 | 4.138 | 6.20 | 4 | 4.138 |
| 1992 | 0.734 | 0.293 | 45 | 4.420 | 4.33 | 3.5 | 4.420 |
| 1727 | 0.553 | 0.263 | 51 | 5.240 | 3.17 | 3 | 5.240 |
| 1571 | 0.446 | 0.202 | 44 | 6.816 | 2.55 | 2.5 | 6.816 |
| $d$ = 714.3 nm, $\bar{d}_1$ = 701.12 nm | | | | | | | |
| $Pb_{1.6}Ge_{19}Sb_{26}Te_{54}$ | | | | | | | |
| 2596 | 0.786 | 0.301 | 51 | 4.232 | 4.99 | 4 | 4.232 |
| 2177 | 0.786 | 0.299 | 42 | 4.266 | 3.88 | 3.5 | 4.266 |
| 1900 | 0.666 | 0.298 | 53 | 4.526 | 3.19 | 3 | 4.526 |
| 1717 | 0.587 | 0.241 | 45 | 5.250 | 2.66 | 2.5 | 5.250 |
| $d$ = 815.2 nm, $\bar{d}_1$ = 766.78 nm | | | | | | | |
| $Pb_5Ge_{12}Sb_{28}Te_{55}$ | | | | | | | |
| 2316 | 0.794 | 0.286 | 41 | 4.352 | 6.12 | 4.5 | 4.673 |
| 2006 | 0.676 | 0.259 | 47 | 4.806 | 5.20 | 4 | 5.111 |
| 1805 | 0.600 | 0.221 | 42 | 5.426 | 4.15 | 3.5 | 5.976 |
| 1616 | 0.341 | 0.186 | 43 | 5.717 | 3.25 | 3 | 6.656 |
| $d$ = 865.6 nm, $\bar{d}_1$ = 798.07 nm | | | | | | | |

The refractive index values obtained can be fit to Wemple DiDomenico (WDD) [17, 18] dispersion relationship. It was the first approach that attached physical significance to the parameters, i.e., to the single oscillator model:

$$\varepsilon_1(\omega) = n^2(\omega) = 1 + \frac{E_o E_d}{E_o^2 - (\hbar\omega)^2} \tag{1}$$

where $\nabla = h/2\rfloor$ ($h$ is Plank's constant), ω is the frequency, $\varepsilon_1(\omega)$ is the real part of the complex electronic dielectric constant ($\varepsilon(\omega) = \varepsilon_1(\omega) + i\varepsilon_2(\omega)$), $E_o$ is the single oscillator energy, which is identified with the mean transition energy from the valence band of lone-pair p-states to conduction band states. $E_d$ is the oscillator strength or dispersion energy. Above equation can be written as:

$$(n^2 - 1)^{-1} = E_o / E_d + (E_o E_d)^{-1}(\hbar\omega)^2 \tag{2}$$

The straight line fitting $(n^2\text{-}1)^{-1}$ vs $(h\omega)^2$ plot enables us to determine $E_o$ and $E_d$ directly from the slope, $(E_o E_d)^{-1}$, and the intercept on a vertical axis, $E_o/E_d$, respectively. The inset in Fig. 2, shows least square fit for $Pb_0Ge_{20}Sb_{24}Te_{56}$ thin film. The straight line equation corresponding to least square fit for $Pb_0Ge_{20}Sb_{24}Te_{56}$ film is, $(n^2\text{-}1)^{-1} = (0.0693 \pm 0.003) - (0.0263 \pm 0.005)\ (h\omega)^2$. The values found for WDD dispersion parameters $E_o$ and $E_d$, calculated from above equation are $E_o$ = 1.63 eV and $E_d$ = 23.61 eV. The WDD refractive index dispersion curves, for the composition $Pb_0Ge_{20}Sb_{24}Te_{56}$ is shown in Fig. 2.

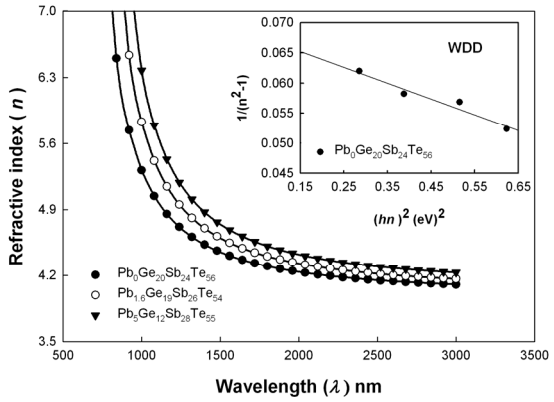


*Fig. 2. The variation of refractive index (n) against wavelength (λ) nm, for Pb:GeSbTe chalcogenide thin films, inset shows the Plot of refractive-index factor $(n^2 - 1)^{-1}$ versus $(h\nu)^2$. $(eV)^2$ for $Pb_0Ge_{20}Sb_{24}Te_{56}$ chalcogenide thin film.*

The absorbance $x$, was obtained using the transmission maxima envelope $T_M(\lambda)$ [16]. The absorption coefficient $\alpha$, of amorphous semiconductors, in the high absorption region, is given according to Swanepoel [14] by the following equation:

$$\alpha = \left(1/d\right)\ln\left(1/x\right) \tag{3}$$

The absorption coefficient $\alpha$, obtained was used to calculate the extinction coefficient $k$ by using relation $k = \alpha\lambda / 4\pi$ . Fig. 3 shows the variation of extinction coefficient $k$ with the wavelength $(\lambda)$. In the high absorption region, involving indirect interband transitions between valence and conduction bands, α follows the relation:

$$\alpha = B(h\nu - E_g^{opt})^2/h\nu \tag{4}$$

where $E_g^{opt}$ is the optical band gap and $B$ is a constant, which is a measure of the extent of band tailing [20]. A plot of $(\alpha h\nu)^{1/2}$ versus $h\nu$ gives a straight line, whose intercept on the energy axis gives $E_g^{opt}$ (Fig. 4).

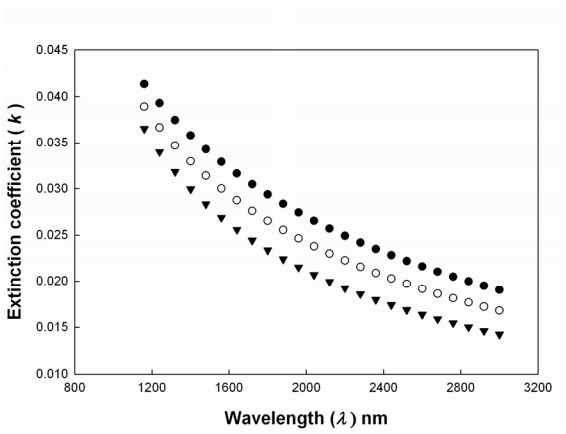


*Fig. 3. The variation of extinction coefficient (k) against wavelength (λ) nm, for Pb:GeSbTe chalcogenide thin films.*

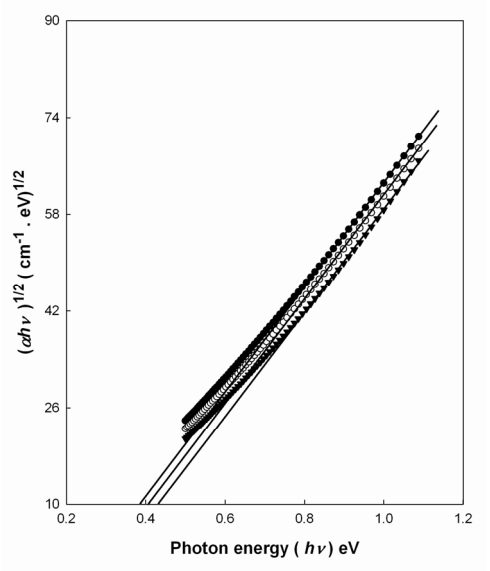


*Fig. 4. Tauc plot for calculating optical gap of Pb:GeSbTe chalcogenide thin films.*

## 4. Discussion

Based on single oscillator model, Wemple and Didomenico put forward a semi-empirical relation for determining the optical parameters at photon energies below the interband absorption edge [17]. Relating the Kramers-Kronig relation [27] for the real part of the dielectric function to relation ($\varepsilon(\omega) = \varepsilon_1(\omega) + i\varepsilon_2(\omega)$), we can have insight into the physical meaning. The parameter $E_o$ and $E_d$ are given by

$$E_o^2 = \frac{M_{-1}}{M_{-3}}$$

and

$$E_d^2 = \frac{M_{-1}^3}{M_{-3}} \tag{5}$$

where $M_{-1}$ and $M_{-3}$ are moments of the $\varepsilon_2(\omega)$ spectrum. Values for $M_{-1}$ and $M_{-3}$ for all compositions under investigation are also given in Table 2. As we can see from equation (5), $E_o$ is independent of the scale of $\varepsilon_2(\omega)$ (the numerator and denominator are of the same power); thus, the oscillator energy is an 'average' energy gap. From Table 2, we can compare the oscillator energy $E_o$ and optical band gap $E_g^{opt}$, and to a good approximation $E_o$ varies in proportion to the optical band gap $E_g^{opt}$, as was earlier found by Wemple and DiDomenico and later by Tanaka, Kosa et al. in AsS chalcogenide system [17,19,22].

*Table 2. Values of oscillator energy ($E_o$), oscillator strength ($E_d$), static refractive index ($n_o$), cation coordination number ($N_c$), optical band gap ($E_g^{opt}$), and moments $M_{-1}$ , $M_{-3}$.*

| Composition | $E_o$ (eV) | $E_d$ (eV) | $n_o$ | $N_c$ | $N_c^{th}$ | $E_g^{opt}$ (eV) | | $M_{-1}$ | $M_{-3}$ |
|---|---|---|---|---|---|---|---|---|---|
| | | | | | | *Present work* | *Ref.* [23] | | |
| $Pb_0Ge_{20}Sb_{24}Te_{56}$ | 1.63 | 23.61 | 3.94 | 3.33 | 3.45 | 0.39 | 0.43 | 14.49 | 5.46 |
| $Pb_{1.6}Ge_{19}Sb_{26}Te_{54}$ | 1.72 | 26.44 | 4.05 | 3.73 | 3.41 | 0.41 | 0.44 | 15.21 | 5.38 |
| $Pb_5Ge_{12}Sb_{28}Te_{55}$ | 1.83 | 30.43 | 4.20 | 4.20 | 3.50 | 0.44 | 0.39 | 16.57 | 5.00 |

Whereas, $E_d$ depends on the scale of $\varepsilon_2(\omega)$ and thus serves as a measure of the strength of interband transitions. The dispersion energy $E_d$, obeys a simple empirical relation,

$$E_d = \beta N_c Z_a N_e, \tag{6}$$

where $\beta$ is a constant, and according to Wemple [18], for 'covalent' crystalline and amorphous materials has a value of $\approx 0.37 \pm 0.05$ eV, $N_c$ is the coordination number of the 'cations' surrounded by 'anion', $Z_a$ is the formal chemical valence of the anion and $N_e$ is the effective number of valence electrons per anion. In particular $Pb_{1.6}Ge_{19}Sb_{26}Te_{54}$, from the value of $E_d$ obtained, and assuming $N_e = (1.6 \times 4 + 19 \times 4 + 26 \times 5 + 54 \times 6)/ 54$ and $Z_a = 2$, the corresponding $N_c$ is $\approx 3.73$. This value is well in agreement with the theoretical coordination number expected, i.e., rewriting the composition under study in $(Pb_{0.035}Ge_{0.4}Sb_{0.57})_{46}Te_{54}$ could be considered as hypothetical cation whose coordination number would be: $N_c^{th} = 0.035 \times 4 + 0.4 \times 4 + .57 \times 3 = 3.41$. From Table 2 we can see that $E_d$ increases with increase in the Pb content. This would mean that the incorporation of Pb into GST increases one or other of the quantities on the right-hand side of equation (6). The incorporation of Pb into the structure results in an increase in the oscillator strength. Since Pb belongs to the same group as that of Ge, thus it appears as a cation in the structure, $Z_a = 2$ remains valid for all samples. As Pb prefers to form covalent bonds in the present structure, thus the nature of chemical bonding remains same, $\beta \approx 0.37 \pm 0.05$ eV also remains valid for all the compositions. For this reason, it is reasonable to assume that average cation coordination is predominately affected by adding Pb to structure. The assumption seems very much true, as we can see a reasonable increase in cation coordination number $N_c$ with Pb addition [Table 2].

Although coordination number $N_c$ is not exactly same, but is very close to theoretically calculated coordination number $N_c^{th}$. Small difference in experimental and theoretical values of coordination number is due to the presence of Ge-Ge and Sb-Sb homopolar bonds, as previously reported by M◁rquez et al. [28]. The accuracy of calculation can also be confirmed by comparing the optical band gap $E_g^{opt}$ calculated in the present work from transmission data with the optical band gap $E_g^{opt}$ calculated using both transmission and reflection data [23].

When a beam of light travels through any material, the electron clouds of the constituent atoms vibrate with oscillating field of light beam at the same frequency. It results in a decrease of the velocity of light through the material ($n = v_{air} / v_{material}$). This means that the refractive index $n$ (the real part), is grater than unity. With increasing frequency the electron clouds of atoms are driven more rapidly and light beam undergoes a further decrease in its velocity, thereby increase in $n$. That is, $n$ decreases with increase in wavelength. Simultaneously, the charge clouds develop an increasingly significant time lag compared with the driving frequency of the light beam and results in some absorption of the light energy. This absorption is expressed as the imaginary part of the refractive index, $k$. The overall refractive index, $N$, is

complex number $N = n + ik$. The compositional dependence of optical parameters is shown in Figure 2, 3 and 4 for all the films under study. It has been observed that the value of refractive index *n* as well as extinction coefficient *k* decreases with increase in the wavelength. A similar trend has also been observed by [24-28]. A slight increase in static refractive index, $n_o = \sqrt{1 + E_d / E_o}$, has been observed with increase in the Pb content as shown in Table 2. This can be explained by the larger electronic polarizability of Pb atoms, with easily polarizable electron clouds having a covalent radius of 147 pm, in comparison with electronic polarizabilities of Ge, Sb and Te atoms with smaller covalent radii of 122 pm, 138 pm and 135 pm, respectively**.** Electronic polarizability can be thought of in terms of the looseness or tightness of the electron charge cloud [29]. The high polarizability means that there is greater displacement as the electron cloud vibrates and the greater driving force of the applied oscillating field, the light, results in greater retardation [29]. A similar explanation has been reported for $(As_{0.33}S_{0.64})_{100-x}Te_x$ and $Ge_xSb_{40-x}S_{60}$ by Marquez et al. [28, 30].

## 5. Conclusions

Swanepoel's method was used to determine the optical constants (*n, k,* and $E_g^{opt}$) for Pb:GeSbTe films. It was necessary to account for the non-uniform thickness of the thin films in order to accurately determine optical properties. The refractive index and the single-oscillator parameters were calculated using WDD method. We found that Pb incorporation results in an increase of refractive index *n*, which is successfully explained with larger electronic polarizability of Pb atoms in comparison to Ge, Sb and Te atoms. Both *n* and *k* were found to decrease with the increase in the wavelength.

## References


[1] J. A. Savage, Infrared optical materials and their antireflection cotings*,* Adam Hilger, Bristol, 1985.

[2] T. Ohta, S. R. Ovshinsky, In: A. V. Kolobov (Ed.), Photo-Induced Metastability in Amorphous Semiconductors, Wiley-VCH, Weinheim, 2003.

[3] A. V. Kolobov, P. Fons, J. Tominaga, A. I. Frenkel, A. L. Ankudinov, S. N. Yannopoulous, K. S. Andrikopoulos, T. Uruga, Jpn. J. Appl. Phys. **44,** 3345 (2005).

[4] M. Popescu, Journal of Ovonic Research **2,** 45 (2006).

[5] M. Popescu, J. Optoelectron. Adv. Mat. **7,** 2189 (2005).

[6] N. Yamada, E. Ohno, K. Nishiuchi, N. Akahira, J. Appl. Phys. **69,** 2849 (1991).

[7] S. Gu, L. Hou, Q. Zhao, R. Huang, Chinese Optics Letters **1,** 716 (2003).

[8] S. W. Ryu, J. H. Oh, B. J. Choi, S. V. Hwang, S. K. Hong, C. S. Hwang, H. J. Kim, Electrochemical and Solid-State Letters **9,** 259 (2006).

[9] A. V. Kolobov, P. Fons, A. I. Frenkel, A. L. Ankudinov, J. Tominaga, T. Uruga, Nature Materials **3,** 703 (2004).

[10] X. J. Lin, L. Bo, S. Z. Tang, F. S. Lin, C. Bomy, Chin. Phys. Lett. **22,** 934 (2005).

[11] K. Wang, D. Wamwangi, S. Ziegler, C. Steimer, M. Wutting, J. Appl. Phys. **96,** 5557 (2004).

[12] K. Wang, C. Steimer, D. Wamwangi, S. Ziegler, M. Wutting, Appl. Phys. A **80,** 1611 (2005).

[13] X. Cheng, L. Bo, S. Z. Tang, F. S. Lin, C. Bomy, Chin. Phys. Lett. **22,** 2929 (2005).

[14] R. Swanepoel, J. Phys. E, Sci. Instrum. **17,** 896 (1984).

[15] M. Abkowitz, Polym. Eng. Sci. **24,** 1149 (1984).

[16] R. Swanepoel, J. Phys. E, Sci. Instrum. **16,** 1214 (1983).

[17] S. H. Wemple, M. DiDomenico, Phys. Rev. B **3,** 1338 (1971).

[18] S. H. Wemple, Phys. Rev. B **7,** 3767 (1973).

[19] K. Tanaka, Thin solid Films **66,** 271 (1980).

[20] J. Tauc, Amorphous and Liquid Semiconductors, Plenum Press, London, 1974.

[21] W. C. Tan, K. Koughia, J. Singh, S.O. Kasap, In: J. Singh (Ed.), Optical Properties of Condensed Matter and Applications*,* John Wiley& Sons, Inc., New York, 2006.

[22] T. I. Kosa, T. Wagner, P. J. S. Ewen, A. E. Owen, Phil. mag. B **71,** 311 (1995).

[23] J. Kumar, M. Ahmad, R. Chander, R Thangaraj, T. S. Sathiaraj, Eur. Phys. J. Appl. Phys. **41,** 13 (2008).

[24] E. R. Shaaban, N. El-Kabnay, A. M. Abou-sehly, N. Afify, Physica B **381,** 24 (2006).

[25] S. M. El-Sayed, Vacuum **72,** 169 (2004).

[26] I. Sharma, S. K. Tripathi, P. B. Barman, J. Phys. D: Appl. Phys. **40,** 4460 (2007).

[27] E. Marquez, J. M. Gonzalez-Leal, R. Jimenez-Garay, S. R. Lukic, D. M. Petrovic, J. Phys. D: Appl. Phys. **30,** 690 (1997).

[28] E. Marquez, A. M. Bernal-Oliva, J. M. Gonzalez-Leal, R. Prieto-Alcon, T. Wagner, J. Phys. D: Appl. Phys. **39,** 1793 (2006).

[29] J. A. Duffy, Phys. Chem. Glasses **42,** 151 (2001).

[30] E. Marquez, J. M. Gonzalez-Leal, A. M. Bernal-Oliva, T. Wagner, R. Jimenez-Garay, J. Phys. D: Appl. Phys. **40,** 5351 (2007).


*Corresponding author: rthangaraj@rediffmail.com